Anisotropic three-dimensional propagation of solar energetic particles in the inner heliosphere

Wolfgang Dröge*, Yulia Kartavykh†, Berndt Klecker‡ and Gennadi A. Kovaltsov†

*Institut für Theoretische Physik und Astrophysik, Universität Würzburg, D-97072 Würzburg, Germany
†Ioffe Physical-Technical Institute, St. Petersburg 194021, Russia
‡Max-Planck-Institut für extraterrestrische Physik, Garching, Germany

Abstract. **We investigate the combined effects of particle propagation parallel and perpendicular to the large-scale magnetic field in the solar wind. Numerical methods employing stochastic differential equations are used incorporating pitch angle diffusion, focusing and pitch-angle dependent diffusion perpendicular to the magnetic field. Spatial distributions of the particles for various combinations of values for the parallel and perpendicular mean free path are presented. Intensity-time histories at different angular distances with respect to the assumed injection region on the Sun are discussed and compared with results of spacecraft observations of solar particles.**

Keywords**: sun, energetic particles, propagation**

I. INTRODUCTION

Interplanetary turbulence plays a crucial role in scattering charged particles, giving rise to transport or diffusion both perpendicular and parallel to the large scale or mean magnetic field, along with drift motions due to large scale gradients. The transport of solar energetic particles parallel to the interplanetary magnetic field can be understood fairly well if it is assumed that only fluctuations with wave vectors parallel to the magnetic field (which account only for 20% or less of the observed fluctuations) effectively scatter the particles, and dynamical effects in the scattering processes are taken into account (see e.g., [1]). Particle transport normal to the average magnetic field is due to the combined effects of particles skipping off a field line, the mixing or random walk of field lines, and concomitant diffusion parallel to the magnetic field. Information about perpendicular diffusion of solar particles can be obtained from observations of cross field gradients which are observed as 'dropouts', 'steps', and 'cutoffs' in the intensity profiles of low-energy ions and electrons in impulsive solar particle events [2] and are believed to be caused by the convection of alternatively filled and empty flux tubes past the spacecraft. These observations indicate a rather small value of the ratio of the perpendicular to parallel diffusion coefficients ($K_\perp/K_\parallel \sim 10^{-4}$). The modulation of galactic cosmic rays and observations of Jovian electrons [3] have suggested $K_\perp/K_\parallel \sim 10^{-2}$. Even values of $K_\perp/K_\parallel \sim 1$, deduced from anisotropy measurements during co-rotating interaction region events have been reported [4]. In the present work we investigate how simulations of the three-dimensional transport of solar particles can be compared with multi-spacecraft observations in order to gain information about particle transport perpendicular to the magnetic field.

II. INTERPLANETARY TRANSPORT

The appearance of solar particle events observed at 1 AU reflects the combination of a number of physical processes. If we consider particles accelerated in solar flares, these processes include acceleration in the flaring region, some kind of lateral transport in the solar corona to a magnetic field line connected with the observer, and transport in the solar wind. In the absence of large-scale disturbances such as CMEs and shocks, the interplanetary magnetic field can usually be described as a smooth average field, represented by an Archimedian spiral, with superimposed irregularities. In this case the transport in the solar wind encompasses the processes focusing, convection and adiabatic deceleration in the diverging solar wind flow, corotation due to $\boldsymbol{E}\times\boldsymbol{B}$ drift, and pitch angle diffusion due to scattering of the particles at magnetic fluctuations embedded in the solar wind which in the limit of strong scattering leads to spatial diffusion. It has become clear in recent years however (see e.g., [1]), that during most solar particle events interplanetary scattering is weak and a theory based on pitch angle scattering should be used to model particle observations (focused transport [5]). Extension to this model have been suggested to include convection and adiabatic deceleration [6] and perpendicular diffusion [7]. Here we consider only particles with sufficiently high energies and omit convection and adiabatic deceleration. The equation to solve then reads:

$$\frac{\partial f}{\partial t}+\mu v\boldsymbol{e_B}\boldsymbol{\nabla}f+\frac{1-\mu^2}{2L}v\frac{\partial f}{\partial \mu}\;-\frac{\partial}{\partial\mu}\left(D_{\mu\mu}(\mu)\frac{\partial f}{\partial\mu}\right)+\boldsymbol{\nabla}(\boldsymbol{K}_\perp\boldsymbol{\nabla}f)\;=\;q(\boldsymbol{r},\mu,t)\quad(1)$$

where $f(\boldsymbol{r},\mu,t)$ is the particle's gyro-averaged phase space density (proportional to the observed particle flux) at the location $\boldsymbol{r}$, v the particle speed, $\mu=\cos\vartheta$ the particle pitch angle cosine, t the time, $L(\boldsymbol{r})$ the focusing length, $D_{\mu\mu}(\boldsymbol{r},\mu)$ the pitch angle scattering coefficient, and $\boldsymbol{K}_\perp$ a tensor describing the diffusion

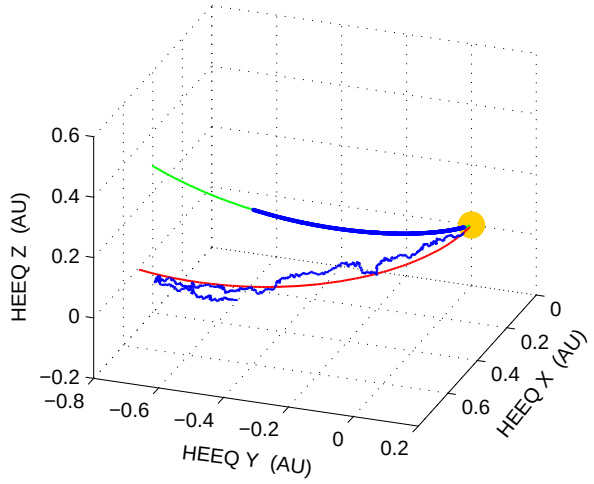

Fig. 1: Particle sample trajectories (thick lines) with (lower) and without (upper) effect of perpendicular diffusion. Thin lines depict magnetic field lines at 70° and 90° co-latitude, respectively.

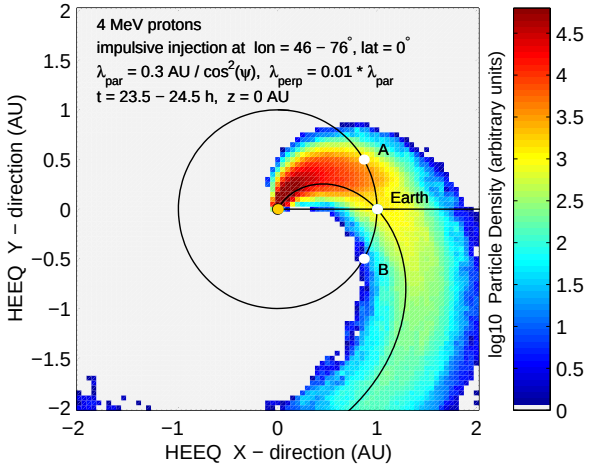

Fig. 2: Distribution of solar protons in the equatorial plane for the specified simulation parameters.

of particles in the two dimensions perpendicular to the ambient magnetic field direction $\boldsymbol{e_B}$. The injection of particles close to the sun is given by $q(\boldsymbol{r}, \mu, t)$. To characterize the strength of the scattering, a diffusion coefficient and a mean free path parallel to the magnetic field ($K_\parallel = v\lambda_\parallel/3$, as well as in the radial direction ($\lambda_r = \lambda_\parallel \cdot \cos^2\psi$, where ψ is the angle between the magnetic field and the radial direction) can be defined with standard methods (see e.g., [1]). Corresponding quantities can also be introduced for the perpendicular transport, i.e., $K_\perp = v\lambda_\perp/3$.

Instead of seeking numerical solutions of the Fokker-Planck equation (1), it is also possible to consider the corresponding Ito stochastic differential equations (SDE) [9]:

$$d\boldsymbol{r}(t) = \mu v dt \boldsymbol{e_B} + \sqrt{2\boldsymbol{K}_\perp}\; d\boldsymbol{W}_\perp(t) + \boldsymbol{\nabla K}_\perp dt \qquad (2)$$

$$d\mu(t) = \sqrt{2D_{\mu\mu}}\; dW_\mu(t) + \left[\frac{v}{2L}(1-\mu^2) + \frac{\partial D_{\mu\mu}}{\partial \mu}\right] dt \qquad (3)$$

which can be solved by means of Monte-Carlo simulations. $W_\mu(t)$ and $\boldsymbol{W}_\perp(t)$ denote one- and two-dimensional Wiener processes, respectively. Both of the above methods have also been extended to include effects of convection and energy losses due to adiabatic deceleration in the expanding solar wind.

III. Simulations

Our simulations require transformations between several coordinate systems: i) the Heliocentric Inertial (HCI) system in which Z is the solar rotation axis, X the solar ascending node on the ecliptic, and Y the third orthogonal axis. We assume that in this system the Sun rotates as a rigid body with an angular velocity Ω, corresponding to a rotation period of 25.4 days, and that the resulting interplanetary magnetic field has the form of Parker Archimedian spirals [8]. In spherical polar coordinates (r, θ, φ) the magnetic field components can then be written as

$$B_r(r,\theta,\varphi) = B_0 \left(\frac{R_\oplus}{r}\right)^2 \qquad (4)$$

$$B_\theta(r,\theta,\varphi) = 0 \qquad (5)$$

$$B_\varphi(r,\theta,\varphi) = B_0 \left(\frac{\Omega\, r}{V_{SW}}\right)\left(\frac{R_\oplus}{r}\right)^2 \sin\theta \qquad (6)$$

where $R_\oplus$ is the solar radius and V_{SW} the solar wind speed.

ii) the co-rotating system which rotates around the Z-axis of system i) with the angular velocity Ω. In this system the solar wind velocity is parallel to the magnetic field and has an absolute value of $V_{SW,cor} = V_{SW}/\cos\psi$.

iii) the co-moving system which moves with the solar wind velocity in system ii). In this system one axis is tangential to the magnetic field line at a given location, the second is normal to the field line and the third orthogonal to the former two.

iv) the Heliocentric Earth Equatorial (HEEQ) system in which compared to the HEEQ system X is replaced by the intersection of the solar equator and the solar meridian as seen from Earth.

The course of the simulation is as follows: a transformation into system ii) is performed in which the quasi-particle undergoes an infinitesimal advective motion along the magnetic field line and stochastic motions in the two dimensions perpendicular to the magnetic field according to the SDE (2), as well a systematic change in μ due to the magnetic mirroring force, according to the SDE (3). After a tranformation into system iii), in which the magnetic fluctuations are at rest, a stochastic change in μ due to pitch angle diffusion, according to the SDE (3), is performed. Then a transformation back to system ii) is made and the cycle repeats. By obeying the proper Lorentz tranformations between the different systems for the quasi-particle it is also possible to take

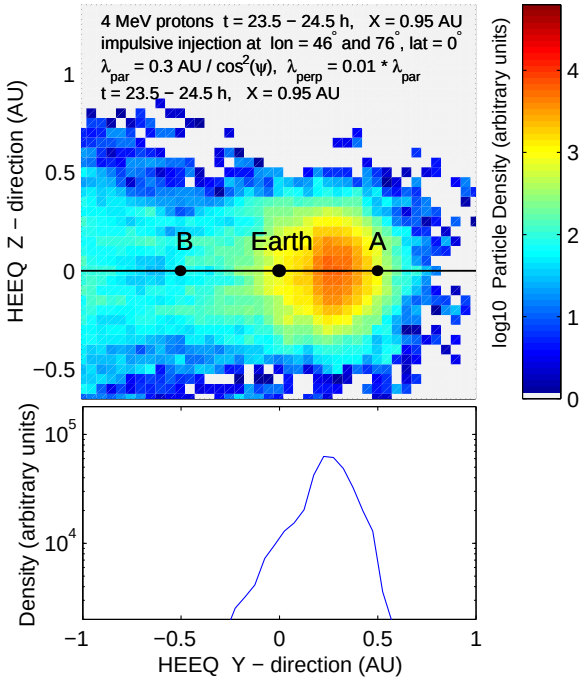

Fig. 3: Distribution of solar protons in a plane perpendicular to the Sun-Earth line (upper panel) and along the HEEQ Y-direction. Details see text.

into account the effects of adiabatic losses in a diverging flow of scattering centers and of convection due to the isotropization of the particle distribution in the system moving with the solar wind (e.g., [10], [11]). At the end a transformation into the HEEQ system for comparison with observations is made which also accounts for the effect of corotation. wind (e.g., [10], [11]).

Figure 1 shows three-dimensional interplanetary magnetic field lines (thin curves) and sample trajectories of quasi-particle spirals (thick lines) for two different values of the polar angle θ, both without the effect of co-rotation. As a test for the accuracy of our numerical method we have left perpendicular diffusion out in the simulation for $\theta = 70°$, for convincing ourselves that the quasi-particle would stay sufficiently close to a given field line. The simulation for $\theta = 90°$ includes perpendicular diffusion.

In order to determine the distribution function of the particles at a given location and time, corresponding to solutions of the equations (1) and (2)/(3), we have to simulate the random walks of a sufficiently large number of quasi-particles and count them in volume elements and time intervals of appropriate size. For the results shown in the following, the number of simulated quasi-particles was $\sim 10^6$, the edge length of a volume box was 0.05 AU, and time intervals were 30 and 60 minutes. Figure 2 shows the distribution of 4 MeV protons $\sim$ 24 hours after an impulsive injection in the equatorial plane. Particles were injected at $r = 0.05$ AU, $\theta = 0°$, $46° \leq \varphi \leq 76°$ with an isotropic pitch angle distribution in the anti-sunward hemisphere. A constant radial mean free path of 0.3 AU (i.e., $\lambda_{\parallel} = 0.3 \text{ AU}/\cos^2\psi$) and a

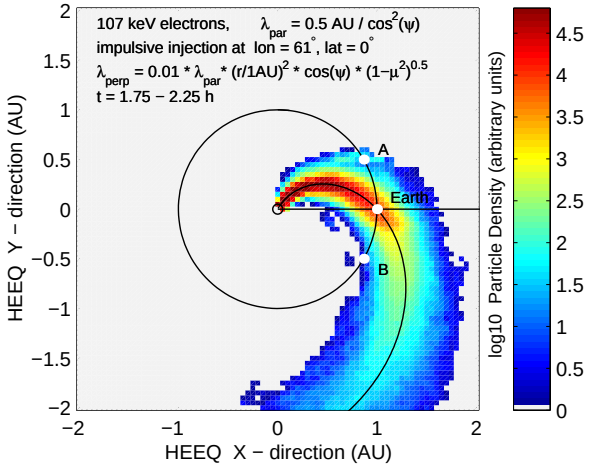

Fig. 4: Distribution of solar electrons in the equatorial plane for the specified simulation parameters.

value of $\lambda_{\perp} = 0.01 \cdot \lambda_{\parallel}$, identical in both perpendicular directions, was assumed. Due to the assumption of a spatially constant $\lambda_{\perp} = 0.003$ AU the particles can diffuse efficiently perpendicular to the field close to the Sun where $\lambda_{\perp}$ is of the order of the extent of the injection length scale. As a result, the particles are distributed over an azimuthal range of $\sim 90°$ at 1 AU. Note also the shift of the ridge of the distribution in azimuth by $\sim 13°$ due to the effect of corotation. To illustrate the possibility of comparing our simulations with multi-spacecraft observations we have indicated here and in Figures 3 and 4 the location of the Earth and two spacecraft at different azimuthal positions (e.g, STEREO-A/B in 2007/2008).

The upper panel of Figure 3 shows the particle distribution in the HEEQ X = 0.95 AU plane. Due to the relatively strong perpendicular diffusion at small r the spread in Z at X = 0.95 AU is almost as much as in Y, in spite of the much narrower injection in θ. The lower panel of the figure shows the density variation along the HEEQ Y - direction for the above value of X. It is obvious that for the parameters assumed here a time variation of the particle flux, resulting from the azimuthal gradient swept over a given spacecraft, cannot explain the observed dropouts or cut-offs.

To investigate the effect of a possibly more realistic spatial variation of $\lambda_{\perp}$ we now assume that it scales with the gyroradius of the particle, i.e., with the magnetic field strength and with the particle's pitch angle:

$$\lambda_{\perp} = 0.01 \cdot \lambda_{\parallel} \cdot \left(\frac{r}{1\text{AU}}\right)^2 \cdot \cos\psi \cdot \sqrt{1-\mu^2} \quad \text{AU} \qquad (7)$$

Figure 4 shows the distribution of 107 keV electrons for the above $\lambda_{\perp}$ at a time of ~ 2 hours after an impulsive injection. As is typical for such electrons, we have assumed a larger parallel mean free path and a narrower injection close to the Sun, i.e., $\lambda_{\parallel} = 0.5 \text{ AU}/\cos^2\psi$ and $\theta = 0°$, $\varphi = 61°$. Because of the stronger magnetic field and also of the fact that the pitch angles are small due to the strong focusing perpendicular diffusion is

Fig. 5: Sketch of two different geometries for particle injection at the Sun. Details see text.

substantially reduced closer to the Sun. Accordingly, the width of the particle distribution perpendicular to the magnetic field at 1 AU becomes significantly narrower.

We will now investigate the effects of a possible perpendicular diffusion on the modeling of intensity-time profiles of particles observed on a single spacecraft. It is important to note that the underlying assumption in fits of particle events using the focused transport equation (1) without perpendicular diffusion was one dimensional transport along the magnetic field line spiral connected to the source and no net loss of particles from that field line, or that particles would be injected uniformly over a cone around a field line from which they could not escape so that there were no perpendicular gradients and perpendicular transport would not matter. With the tools developed here we can now study more realistic cases. The sketch in the left panel of Figure 5 illustrates the situation where particles are injected over a limited azimuthal range and perpendicular diffusion is taken into account. Some time after the injection the particle intensity at a location indicated by the dot will drop due to escape of particles along the field line but in addition also due to diffusion perpendicular to the field. The middle curve in Figure 6 shows the resulting prediction from our simulation assuming a spatial variation of $\lambda_\perp$ as in equation (7), but for 4 MeV protons, $\lambda_\parallel = 0.5\ \mathrm{AU}/\cos^2\psi$ and a ratio $\lambda_\perp/\lambda_\parallel$ = 0.0005 at 1 AU and for μ = 0. Compared to the prediction of the one-dimensional propagation model for the same value of $\lambda_\parallel$ the intensity drops significantly faster after the maximum. The sketch in the right panel of Figure 5 depicts the situation where the field line connected with the observer is 5° away from the boundary of the injection range at the time of the particle injection and leaves the injection range after $\sim$ 7 hours due to co-rotation. The corresponding time profile from the simulation is shown as the lower curve in Figure 6. The sudden drop (indicated by the arrow) marks the transition to the time after which particles are around only because of perpendicular diffusion out of the injection range. The steepness of the gradient is of the order of the observed dropouts and cutoffs in impulsive particle events.

IV. Summary

We developed a numerical model to solve the equation describing anisotropic three-dimensional propagation of solar energetic particles in the inner heliosphere. The model includes the effects of pitch angle scattering,

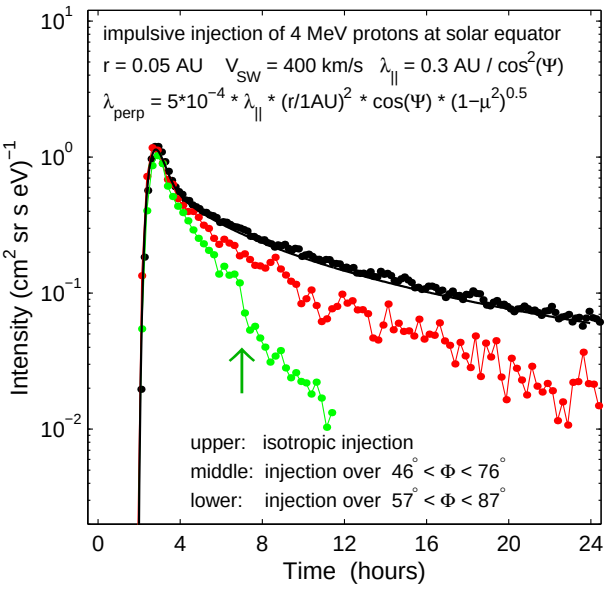

Fig. 6: Intensity profiles of solar protons for different injection and propagation conditions. Details see text.

diffusion in two dimensions perpendicular to the ambient magnetic field, focusing, and injection over a finite range of pitch angles, and solar longitude and latitude. First results for 100 keV electrons and 4 MeV protons show that realistic results can be obtained when we assume that the perpendicular diffusion scales in the inner heliosphere with the gyroradius of the particle. Step-like intensity decreases as frequently observed at 1 AU can be reproduced for a ratio of $K_\perp/K_\parallel \sim 5\cdot10^{-4}$. The model can easily be extended to lower energies by including the effects of convection and adiabatic deceleration. The model provides an ideal tool to investigate more realistically as it was possible in the past solar energetic particle injection and propagation, using multi-spacecraft observations separated in both solar longitude and latitude as available from, for example, ACE, Ulysses, and STEREO.

V. Acknowledgements

Y.K. and G.K. thank the Russian Foundation for Basic Research for partial support (project No 09-02-00019-a).

References

[1] W. Dröge, ApJ 589, 1027, 2003
[2] J. Giacalone and J. R. Jokipii, ApJ 532, L75, 2000
[3] Conlon , J. Geophys. Res. 83, 541, 1978
[4] J.R. Dwyer et al., ApJ 490, L115, 1997
[5] E. C. Roelof, Propagation of solar cosmic rays in the interplanetary magnetic field, in *Lectures in High Energy Astrophysics*, edited by H. Ögelmann, H., and J. R. Wayland, p. 111, NASA SP-199, 1969.
[6] D. Ruffolo, ApJ 442, 861, 1995
[7] M. Zhang, G. Qin and H. Rassoul, ApJ 692,109, 2009
[8] E. N. Parker, *Interplanetary Dynamical Processes*, New York: Wiley and Sons, 1963
[9] C. W. Gardiner, *Handbook of Stochastic Methods*, Berlin: Springer, 1983
[10] L. Kocharov, R. Vainio, G.A. Kovaltsov and J. Torsti, Solar Phys. 182, 195, 1998
[11] W. Dröge, Y.Y. Kartavykh, B. Klecker and G.M. Mason, 2006, ApJ 645, 1516, 2006